Prepared for submission to JINST

14TH topical Seminar on Innovative Particle and Radiation Detectors
3 - 6 October 2016
Siena, Italy

The LHC Run 2 ATLAS Trigger System: Design, Performance and Plans

M. zur Nedden on behalf of the ATLAS collaboration

Humboldt-Universität zu Berlin, Institut für Physik,
Newtonstraße 15, 12489 Berlin, Germany

E-mail: nedden@physik.hu-berlin.de

Abstract: In many high-energy physics experiments, online selection is vital to collect the most interesting collisions out of the large data volume. The ATLAS experiment at the Large Hadron Collider (LHC) utilizes a trigger system that consists of a hardware Level-1 (L1) and a software based high-level trigger (HLT), reducing the event rate from the LHC bunch-crossing rate of 40 MHz to an average recording rate of around 1000 Hz. In Run 2 of the LHC, starting in spring 2015, the LHC is operating at a centre-of-mass energy of 13 TeV providing an instantaneous luminosity up to $1.2 \cdot 10^{34}\,\mathrm{cm}^{-2}\mathrm{s}^{-1}$. The ATLAS trigger system has to cope with these challenges, while maintaining or improving upon the efficiency to select relevant physics processes. In this paper, the ATLAS trigger system for the LHC Run 2 is reviewed. Secondly, the impressive performance improvements in the HLT trigger algorithms used to identify leptons, hadrons and global event quantities like missing transverse energy is shown. Electron, muon and photon triggers covering transverse energies from a few GeV to several TeV are essential for signal selection in a wide variety of ATLAS physics analyses to study Standard Model (SM) processes and to search for new phenomena. Finally, further developments planned for the rest of the LHC Run 2 are discussed. These include two new hardware subsystems for topological selections at L1 and full-scan tracking at the input to the HLT.

Keywords: Trigger, DAQ

ArXiv ePrint: 2016.abcdef

ATL-DAQ-PROC-2016-039
10 December 2016

Contents

1 ATLAS Trigger Overview

The trigger and data acquisition system (TDAQ) is an essential component of any collider experiment as it is responsible for deciding whether or not to keep an event from a given bunch-crossing for later study. Furthermore, triggering in a high density hadronic environment such at the LHC is a very challenging task. The high instantaneous luminosities of up to $L = 1.2 \cdot 10^{34}\,\mathrm{cm}^{-2}\mathrm{s}^{-1}$ lead to very high trigger rates and the high pile-up of multiple interactions per bunch-crossing of up to a mean of $\langle\mu\rangle \approx 35$ causes high occupancy in the detector (Fig.1). An efficient and reliable trigger and data acquisition system is required to cope with such beam conditions which result in large and complex data flows. However, a high selectivity in terms of the trigger performance is as important as a high signal purity and trigger efficiency. For a successful data taking, a good balance between low thresholds and high trigger rates must be found, given the limited bandwidth in the online and offline computing resources. For the ATLAS [1] TDAQ system, complex selection strategies were developed and successfully implemented. A reliable early data reduction is crucial for a successful physics program, with respect to the typically high rate of background processes in hadronic collisions.

pp-interactions at LHC energies of $7 - 13\,\mathrm{GeV}$ provide a challenging environment for trigger operation. The ATLAS trigger and data acquisition system was very successful in the LHC Run-1, but needed to be adapted to the more challenging conditions of LHC Run 2. Many improvements and fundamental modifications were made during the shutdown. The commissioning phase at the start of LHC Run 2 in spring of 2015 was very efficient and fast, leading to a stable and reliable running of the ATLAS trigger system.

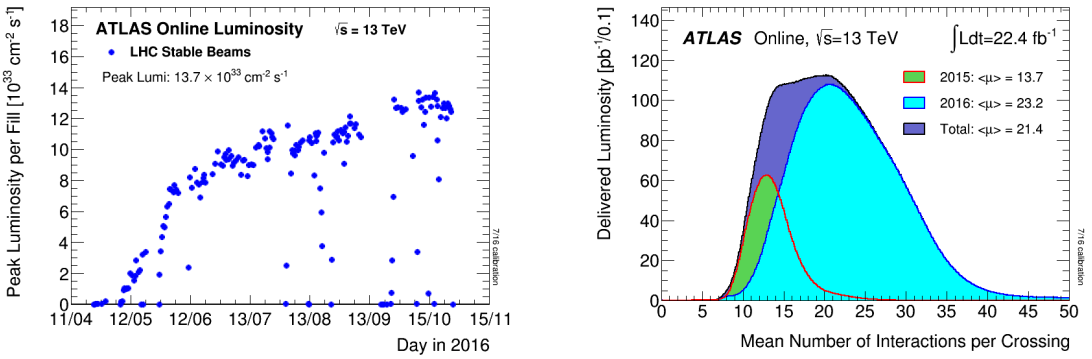

Figure 1. (Left) The peak instantaneous luminosity delivered to ATLAS during stable beams for pp collisions at 13 TeV centre-of-mass energy is shown for each LHC fill as a function of time in 2016. (Right) luminosity-weighted distribution of the mean number of interactions per crossing for the 2015 and 2016 pp collision data [2].

1.1 Trigger Functionality

The ATLAS trigger system consists of two independent levels, a hardware-based first level (L1) and a software-based high level trigger (HLT). The L1 trigger is implemented in fast custom-made electronics and runs with a fixed latency of 2.5 μs. L1 reduces the event rate from the LHC interaction rate of 40 MHz to $\approx$ 100 kHz. Up to 512 decision items are built, based on Regions of Interest (RoI) in η/ϕ retrieved from the muon (L1Muon) and calorimeter (L1Calo) systems. The L1 trigger decision is formed by the Central Trigger Processor (CTP). All three systems were upgraded and improved for LHC Run 2 and a new component, the topological trigger (L1Topo) was included. The L1Topo trigger performs selections based on geometric or kinematic association between trigger objects received from L1Calo or L1Muon and was commissioned recently (see Sec. 3.1 and 3.2). Another new system is the Fast Tracker (FTK), which provides hardware-based tracking information at the rate of the events accepted by L1 for later usage in the HLT. Both of these are crucial for the ATLAS TDAQ system to cope with the anticipated higher luminosities of the LHC up to $1.5 \cdot 10^{34}\,\mathrm{s}^{-1}\mathrm{cm}^{-2}$.

In the HLT, offline-like reconstruction algorithms run in a large farm of $\approx$ 40.000 processor cores and a decision is formed typically within 300 ms. The HLT is a software trigger providing typically 2500 independent trigger chains. These are sequences of offline-like algorithms executed within the L1 RoIs, and higher precision reconstruction is performed later in the sequence. Event building takes place at a flexible point within the event processing, ensuring an optimal usage of the farm and DAQ network resources. Furthermore, full-event reconstruction is possible at the HLT. Events accepted by the HLT are written into different data streams (Fig. 2) to be used for physics analysis, trigger level analysis, monitoring or detector calibration. Depending on the data stream, the full event (e.g. for physics analysis) or only partial event information (e.g. for detector calibration, monitoring or trigger level analysis) is written out, allowing for higher rates without consuming a significant amount of the available bandwidth.

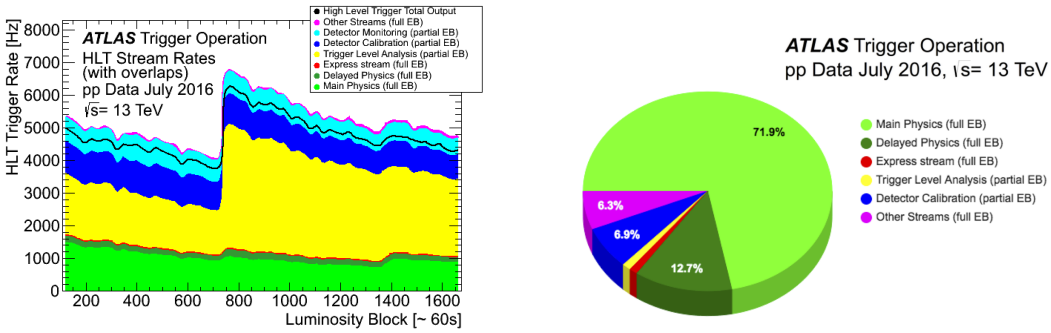

Figure 2. (Left) HLT stream rates as a function of the number of luminosity blocks (which last 60 s on average), in a fill taken in July 2016 with a peak instantaneous luminosity of $1.2 \cdot 10^{34}$ cm^{-2}s^{-1} and an average (peak) pile-up of 24.2 (35). Stream overlaps are only accounted for in the HLT total output rate, displayed by the black line. (Right) Contribution of the HLT streams the total output bandwidth for the same fill [4].

1.2 Trigger Menu

The trigger menu defines the configuration of the full L1 and HLT decision making process [3]. L1 items are connected to HLT chains and chains to data streams. The trigger menu consists of primary triggers used for physics measurements; support triggers used for efficiency and performance measurements or monitoring; alternative triggers running alternative online reconstruction algorithms as primary or support selections; backup triggers with tighter selections and lower expected rates for use in case of an increase in instantaneous luminosity or other changes in data-taking conditions and finally calibration triggers, running at high rate but storing very small events using partial-event building. On top of the trigger menu, prescale factors for L1 items and HLT triggers are a crucial part of the trigger configuration. Prescale factors are used to reduce the amount of events accepted by a certain L1 item or HLT chain. For a prescale factor of N, only one event out of N events which fulfill the trigger requirement is accepted. Individual prescale factors can be given to each chain at each trigger level. Whereas the primary triggers are typically un-prescaled, the support, alternative and backup trigger are kept at reasonable low rate via the application of appropriate prescale factors. The trigger menu composition ensures a high acceptance for physics events (e.g. beyond the SM (BSM) / Super Symmetry (SUSY) / Higgs / SM / top physics) while simultaneously collecting relevant information for detector calibration and monitoring, and always respects the limits of the TDAQ system. As is observed in Fig. 2, the largest bandwidth consumption originates from the main physics stream.

According to the expected performance of the LHC, the trigger menu composition is optimised for several luminosity points. Since trigger rates normally scale linearly with the luminosity, the menu composition must be adapted to the expected instantaneous luminosity. If the luminosity has decayed sufficiently from its peak value, additional triggers are enabled and decreased prescale factors are applied to make maximal use of the available bandwidth. In order to guarantee stable running, a change of the trigger composition is done via sets of prescale factors predefined for certain luminosities. Dedicated triggers can also be disabled via the prescale factors.

The ATLAS trigger menu at L1 is based on candidate objects identified within a RoI. Candidates are of type muons (MU), electromagnetic clusters (EM), jets (JET) or tau (TAU). Additionally, global

sums of missing transverse energy (XE) and total energy (TE) are constructed. The allocated rate in the main physics stream for triggers derived from combinations of these objects is shown in Fig. 3. At the HLT, the L1 decisions are revised and more sophisticated selections are applied, leading to triggers on physics objects such as muons, electrons, photons, jets, b-jets, missing transverse energy, taus and b-hadrons (Fig. 3). Multi-object triggers are additionally formed at both levels. To ensure the highest possible physics output and the stability of the system, a good balance between the choice of thresholds, isolation criteria, multiplicities and prescale factors must be found. Given the complexity of the menu, dedicated tools are utilized to validate the trigger algorithms to ensure the menu is working optimally for the current LHC luminosity before it is deployed online. There are dedicated trigger menus for pp-collisions, for Heavy-Ion data taking and for special runs, e.g. cosmics or Van-der-Meer scans.

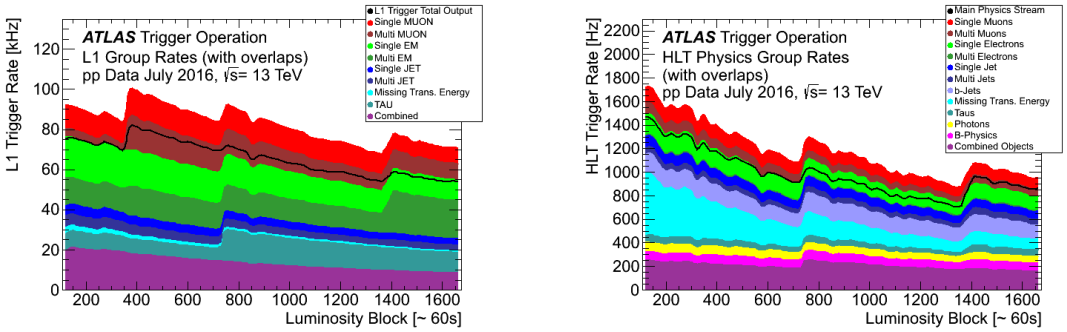

Figure 3. L1 (left) and HLT (right) physics trigger rates grouped by trigger signatures as a function of the luminosity block number, in a fill taken in July 2016 with a peak instantaneous luminosity of $1.2 \cdot 10^{34}$ cm^{-2}s^{-1} and an average (peak) pile-up of 24.2 (35). Due to overlaps, the sum of the individual group rates is higher that the total L1 rate (left) and *Main* physics stream rate (right), which are shown as black lines. The rates periodically increase due to change of prescale factors to optimise resource usage [4].

2 ATLAS Trigger Performance

The performance of the the ATLAS trigger is evaluated by the appropriate trigger groups based on physics objects as described in Sec. 1.2. Some trigger chains used for specific physics channels are: electron / photon triggers for Higgs, top (electron), SM and SUSY studies; tau triggers for Higgs and BSM studies; jet/ b-jet triggers for top, Higgs and SM studies; missing transverse energy triggers for BSM and SUSY studies and muon triggers for top, SM, B-physics and SUSY studies. In this chapter, a brief overview of the performance of the different trigger groups is given.

2.1 Electron, Photon and Tau Trigger

The electron, photon and tau trigger performance was studied in detail on data and the efficiency was measured as a function of the reconstructed transverse momentum p_{T} (for e, τ) or the transverse energy E_{T} (for γ). The electron selection uses a likelihood-based identification, whereas photon identification relies only on cuts applied on shower shape variables. In the trigger, only hadronic decaying taus (τ_{had}) are considered, here a boosted decision tree (BDT) technique is used. Leptonic

tau decays are covered by the respective single-lepton triggers (e/μ). The trigger identification efficiency shows steep turn-on regions as a function of p_{T} or E_{T} with a plateau at $\epsilon \approx 100\,\%$ for all three trigger objects. The data are well described by Monte Carlo simulation as is seen in the comparisons based on the tag-and-probe method using a sample of simulated $Z \to ee/\tau\tau$ event. All results are shown in Fig. 4.

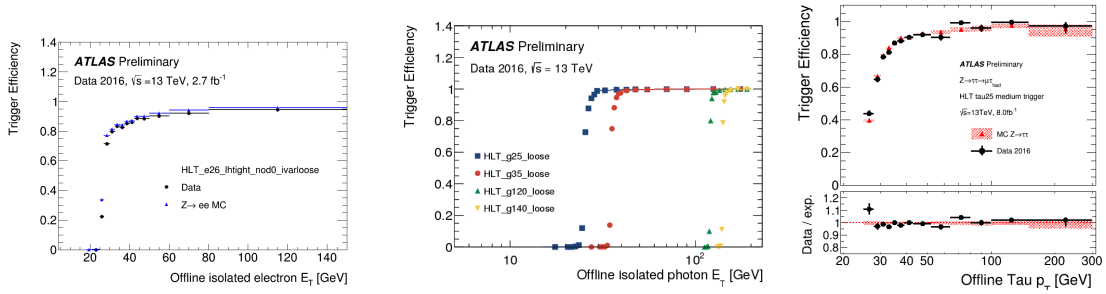

Figure 4. (Left) Efficiency of the `HLT_e26_lhtight_nod0_ivarloose` trigger as a function of the offline electron candidate's transverse energy (E_{T}) requiring an electron candidate with $E_{\mathrm{T}} > 26\,\mathrm{GeV}$ which satisfies the likelihood-based tight identification criteria without applying transverse impact parameter requirements, but applying variable-size cone isolation. (Middle) Efficiency of photon triggers requiring a transverse energy $E_{\mathrm{T}} > 25\,\mathrm{GeV}$ (blue squares), 35 GeV (red circles), 120 GeV (green triangles) and 140 GeV (yellow triangles) and loose photon identification criteria as a function of the transverse energy of the photon candidates as reconstructed offline. Here the candidates are required to pass the tight identification selection with $|\eta| < 2.37$, excluding the transition region between the central and forward electromagnetic calorimeters at $1.37 < |\eta| < 1.52$. [5]. (Right) Tau trigger efficiency measured in data and compared to simulation, with respect to offline reconstructed tau candidates with one or three tracks which pass the offline medium identification criteria, plotted as function of the offline transverse momentum. The trigger efficiency is measured in a tag and probe analysis with $Z \to \tau\tau \to \mu\tau_{\mathrm{had}}$ events. The corresponding online tau requirements are a transverse momentum above 25 GeV, between one and three tracks, and to pass the online medium identification [6].

2.2 Jet and Missing Transverse Energy Trigger

Major improvement of the jet-trigger for the LHC Run 2 has been achieved during the shutdown. The jet-trigger is now able to use the data from the entire calorimeter necessary for the anti-k_{T} algorithm due to improvements to the speed of calorimeter clustering algorithms by a factor of 2, and of the calorimeter data unpacking by a factor of 7. This is made possible mainly due to the upgraded read-out system being capable of delivering event-data at higher rate. As a result, the jet trigger algorithms at the HLT are able to perform a full-scan of the detector. The efficiency of several HLT jet triggers as a function of the offline reconstructed jet transverse momentum, p_{T}, is shown in Fig. 5 (left). A sharp turn-on is observed over a very large jet-p_{T} range due to a good agreement between the energy scale of HLT and offline jets.

Pile-up mitigation is the main challenge for missing transverse energy triggers ($E_{\mathrm{T}}^{\mathrm{miss}}$) since their rates are severely affected by detector noise, miss-measurements and pile-up, resulting in their rates increasing faster than linearly with increasing pile-up. At the HLT, several reconstruction algorithms have been implemented. Currently the so-called `mht`-algorithm, reconstructing $E_{\mathrm{T}}^{\mathrm{miss}}$ by summing the $-p_{\mathrm{T}}$ of the HLT jets, is the default, as it was shown to provide the best performance.

The pile-up effects of the $E_{\mathrm{T}}^{\mathrm{miss}}$ trigger derive mainly from the utilisation of information from all of the calorimeters. The efficiency as a function of the offline reconstructed transverse missing energy is plotted in Fig. 5 (right) for several HLT $E_{\mathrm{T}}^{\mathrm{miss}}$ triggers algorithms, along with a L1 item requiring $E_{\mathrm{T}}^{\mathrm{miss}} > 50\,\mathrm{GeV}$. A steep turn-on and an efficiency plateau at 100 % is observed.

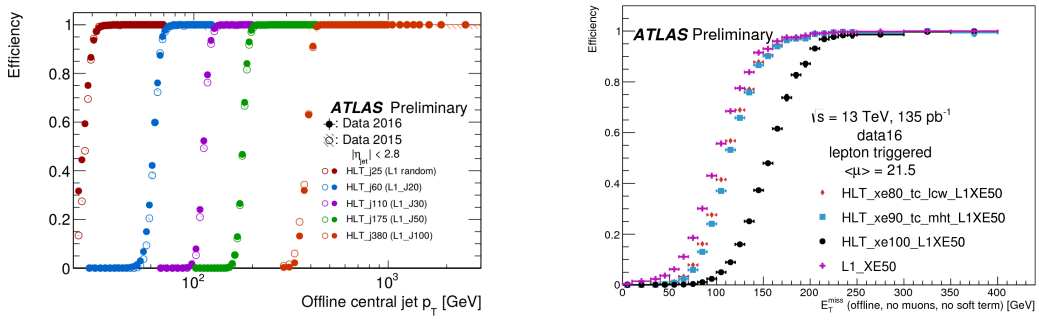

Figure 5. (Left) Efficiencies for HLT single-jet triggers are shown as a function of the leading offline jet p_{T} for jets with $|\eta| < 2.8$. Triggers denoted `HLT_jX` accept an event if a jet is reconstructed at the HLT with $E_{\mathrm{T}} > X\,\mathrm{GeV}$. The un-prescaled trigger with the lowest threshold requires a jet with $E_{\mathrm{T}} > 380\,\mathrm{GeV}$ at the HLT (`HLT_j380`). Triggers in 2016 (filled circles) become fully efficient at the same point as was observed in 2015 (open circles), despite higher levels of pileup. The L1 seed trigger for each HLT item is shown in parenthesis; 'L1 random' denotes that events are randomly accepted at L1. Events used to measure the performance of each trigger are selected from fully-efficient, lower-threshold jet triggers [7]. (Right) Efficiency as a function of modified offline $E_{\mathrm{T}}^{\mathrm{miss}}$ for three different trigger algorithms as a function of the offline $E_{\mathrm{T}}^{\mathrm{miss}}$. Three different $E_{\mathrm{T}}^{\mathrm{miss}}$ HLT algorithms are shown. All three algorithms are seeded by a L1 trigger algorithm with a nominal threshold of 50 GeV which is also shown [8].

2.3 Muon Trigger

Major improvements were made to the muon triggers for LHC Run 2, a new coincidence logic at L1 suppresses fake triggers in the forward region. The coverage of the L1 muon trigger detectors in the central region was increased by 4 % with newly installed chambers in the so-called feet region of the muon system. In Fig. 6 a sharp turn-on curve is observed reaching an HLT efficiency with respect to L1 of $\epsilon = 100\,\%$.

2.4 B-Physics Trigger

B-physics triggers are mainly based on di-muon trigger (Fig. 7, right): $4 + 4\,\mathrm{GeV}$, $4 + 6\,\mathrm{GeV}$ or $6 + 6\,\mathrm{GeV}$ di-muon candidates at L1 which are then confirmed at the HLT. The single-μ trigger is based on a threshold of 15 GeV at L1 seeding a 20 GeV threshold muon-chain at the HLT. Without further requirements, too large a rate would be obtained at high instantaneous luminosities leading to the need for large prescale factors. Considering searches for very rare BSM decays such as $B_s^0 \to \mu\mu$, this would make the ATLAS B-physics program impossible. Accordingly, the usage of the L1Topo trigger (see Sec. 3.1) is vital to reduce the di-muon trigger rates while retaining sensitivity for the BSM physics program. This is shown in Fig. 7 (left): a reduction of the rate by the L1Topo trigger compared to the `L1_2MU` only trigger is clearly visible using a signal sample of $B_s^0 \to \mu\mu$.

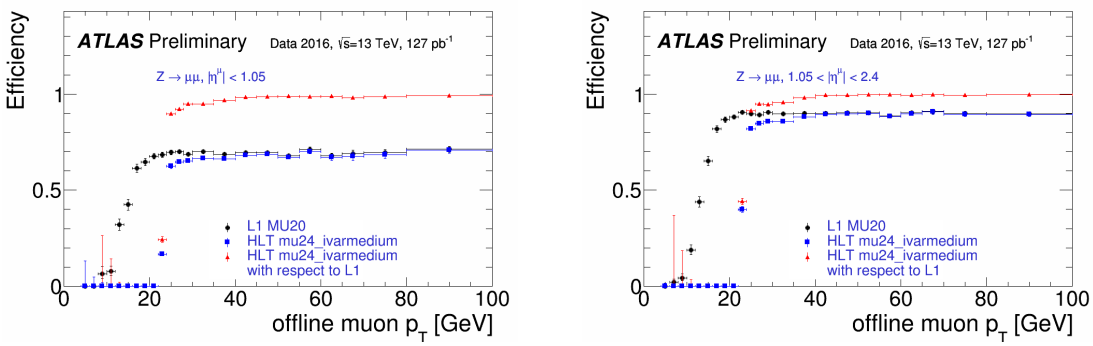

Figure 6. Absolute efficiency of the L1 `MU20` trigger and absolute and relative efficiencies of `mu24_ivarmedium` at the HLT, plotted as a function of p_{T} of offline muon candidates in the central (left) and forward (right) detector region. The efficiency is computed with respect to offline isolated muon candidates which are reconstructed using the standard ATLAS software and which are required to pass a medium quality requirement. The `MU20` trigger requires that a candidate passed the 20 GeV threshold requirement of the L1 muon trigger system. The `mu24_ivarmedium` trigger is seeded by the `MU20` trigger and is required to satisfy a 24 GeV HLT threshold and to pass a medium isolation selection computed using inner detector tracks reconstructed online by the HLT within a cone with a variable size, which depends on the p_{T} of the muon. The efficiency is measured using a tag-and-probe method with $Z \to \mu\mu$ candidates, with no background subtraction applied. Only statistical data uncertainties are shown [9].

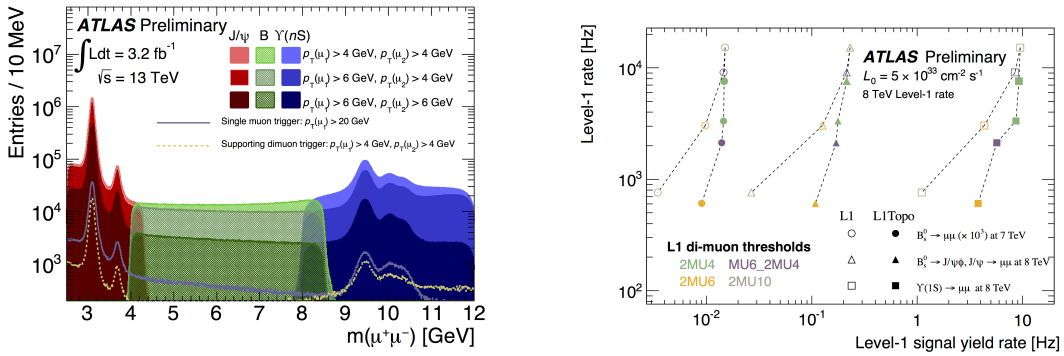

Figure 7. (Left) Invariant mass distributions for oppositely charged muon candidate pairs that pass various triggers. The di-muon triggers require two muons at L1, passing thresholds of $p_{\mathrm{T}} > 4$ GeV or 6 GeV , which are confirmed at the HLT. Pairs of oppositely charged muons are fit to a common vertex, using the inner detector track parameters and invariant mass requirements to restrict events to the charmonium, b-hadron and bottomonium invariant mass ranges. For comparison, the lowest threshold un-prescaled single muon trigger is shown. (Right) Estimated L1 background and signal yield rates, at a reference instantaneous luminosity $L_0 = 5 \cdot 10^{33}\,\mathrm{cm}^{-2}\mathrm{s}^{-1}$, for the LHC Run 2 Heavy Flavour L1Topo menu (filled markers) and existing di-muon only triggers (empty markers). [10].

3 New ATLAS Trigger Subsystems

3.1 L1 Topological Trigger

There are severe limitations on the ATLAS TDAQ system affecting its performance at luminosities above $\approx 1.5 \cdot 10^{34}\,\mathrm{cm}^{-2}\mathrm{s}^{-1}$ due to the increased trigger rate caused by higher pile-up. In order to guarantee the stable running of the system, either additional prescale factors or an increase of the trigger thresholds would be needed. However, this would reduce the physics acceptance, counteracting the gain of the higher luminosities. Therefore, the L1 topological trigger (L1Topo) is crucial to make full use of the luminosity upgrade. The L1Topo trigger decision is derived from topological combinations of trigger objects identified by L1Calo and L1Muon. Up to 128 configurable algorithms are available programmed into Field Programmable Gate Arrays (FPGAs). These combine calorimeter and muon L1 triggers allowing for selections on complex physics quantities such as angular distances (η, ϕ, $\Delta\eta$, $\Delta\phi$, ΔR; missing, transverse and invariant mass calculations; compound triggers such as e/γ, jets, μ, τ, $E_{\mathrm{T}}^{\mathrm{miss}}$ and $H_{\mathrm{T}} = \Sigma(p_{\mathrm{T}})$). The L1Topo trigger is a physics oriented system providing dedicated triggers for specific physics channels. In Fig. 8, the results of commissioning the L1Topo H_{T} trigger is shown. The efficiency turn-on curve as a function of the reconstructed H_{T}, the scalar sum of jet-p_T, shows the expected behaviour. Also the expected trigger rates as a function of the instantaneous luminosity for two L1Topo H_{T} triggers compared to online measured rates are show. Both the prediction and the online rates agree and exhibit linear scaling with instantaneous luminosity. Such validation is a prerequisite to the use of L1Topo in active selection mode. Good progress has been made, therefore the L1Topo trigger system is ready to be used in selective mode.

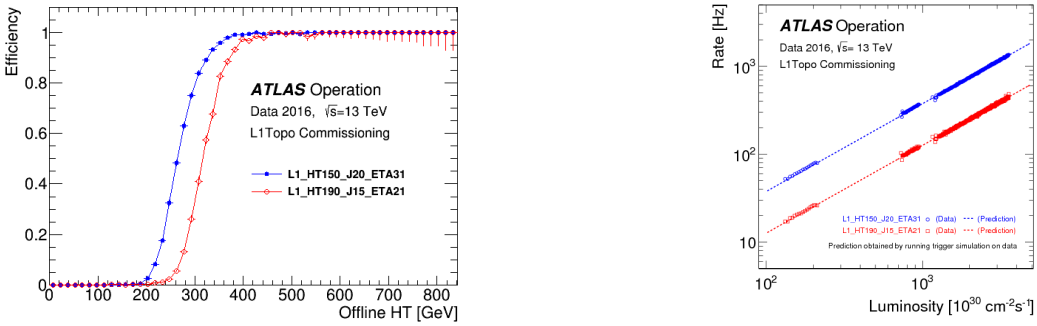

Figure 8. (Left) The efficiency turn-on curves for two L1Topo triggers based on the H_{T} algorithm as a function of the offline-reconstructed H_{T}, the transverse energy sum of jets. The `HT150_J20_ETA31` (`HT190_J15_ETA21`) requires the transverse energy sum of jets with $p_{\mathrm{T}} > 20(15)$ GeV and pseudo-rapidity $|\eta| < 3.1(2.1)$ to be above 150(190) GeV. (Right) Trigger rates as a function of the instantaneous luminosity of two L1Topo triggers based on the H_{T} algorithm, for the same trigger selection as on the left plot. The online trigger rates are compared to the prediction obtained by running the trigger simulation on an un-biased data sample. [4].

3.2 Fast TracKer

The usage of tracking information at the trigger level is very challenging. Currently, at L1 there is no tracking information available. Tracking information is instead initially reconstructed with RoIs during the HLT processing. To overcome this, a hardware-based track finder, the Fast TracKer (FTK), performs a global track reconstruction for tracks with $p_{\mathrm{T}} > 1\,\mathrm{GeV}$ using silicon trackers information. The FTK provides the full-event track information to the HLT at the full L1 acceptance rate of up to $\approx 100\,\mathrm{kHz}$ by using associate memory for pattern matching and FPGAs for track fitting. As is observed in Fig. 9, the refitted FKT-tracks show a good level of agreement with offline reconstructed tracks in both heavy- and light-flavour jets. The FKT exhibits good pile-up robustness and will be used for secondary-vertex finding for heavy- flavour physics. Currently, installation and online tests of the FTK are ongoing with the prospect of the system actively participating in event selection from 2017 on.

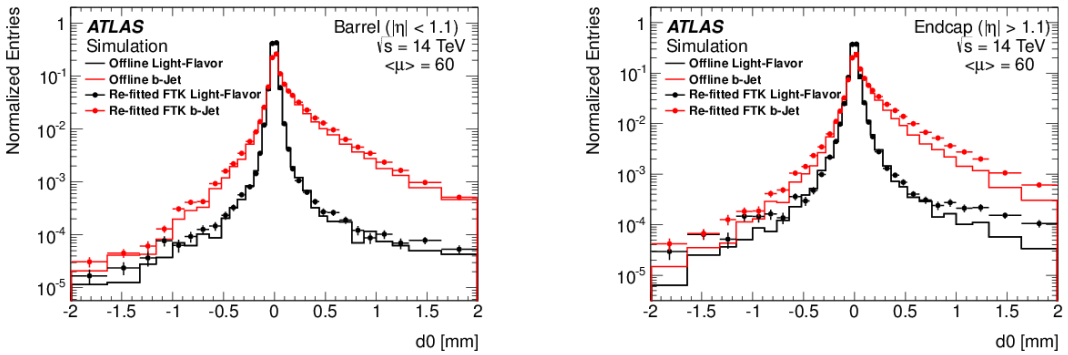

Figure 9. The transverse impact parameter is shown for offline tracks associated to light-flavor (black) and heavy-flavor (red) jets. The solid lines show the distribution foroffline tracks, whereas the points show the re-fitted FTK tracks in the central (left) and forward (right) region. The transverse impact parameter significance is defined as the transverse impact parameter divided by its associated uncertainty. The impact parameter is signed such that track displacements in the direction of the jet have positive values, while tracks with displacements opposite of the jet direction are negative [11].

4 Summary and Outlook

The Run 2 requirements at the LHC are challenging for the ATLAS trigger system. As demonstrated, the ATLAS trigger system is prepared to cope efficiently and reliably within the LHC Run 2 physics environment. The major improvements and upgrades made for LHC Run 2 are performing well and are an important for the success operation of the ATLAS trigger system. The trigger menu is meeting all the physics performance requirements as is illustrated in extensive studies of the trigger performance. Further ongoing developments include the L1 topological trigger which is in a commissioning phase and the the Fast TracKer which is in a testing phase. By utilising both of these systems, the ATLAS trigger will maintain a high physics performance at even higher instantaneous luminosities.

References

[1] 2008 JNST 3 S08003, The ATLAS Collaboration

[2] [https://twiki.cern.ch/twiki/bin/view/AtlasPublic/LuminosityPublicResultsRun2]

[3] ATL-DAQ-PUB-2016-001, The ATLAS Collaboration

[4] [http://twiki.cern.ch/twiki/bin/view/AtlasPublic/TriggerOperationPublicResults]

[5] [https://twiki.cern.ch/twiki/bin/view/AtlasPublic/EgammaTriggerPublicResults]

[6] [https://twiki.cern.ch/twiki/bin/view/AtlasPublic/TauTriggerPublicResults]

[7] [https://twiki.cern.ch/twiki/bin/view/AtlasPublic/JetTriggerPublicResults]

[8] [https://twiki.cern.ch/twiki/bin/view/AtlasPublic/MissingEtTriggerPublicResults]

[9] [https://twiki.cern.ch/twiki/bin/view/AtlasPublic/MuonTriggerPublicResults]

[10] [https://twiki.cern.ch/twiki/bin/view/AtlasPublic/BPhysicsTriggerPublicResults]

[11] [https://twiki.cern.ch/twiki/bin/view/AtlasPublic/FTKPublicResults]